IJNRD.ORG ISSN : 2456-4184
INTERNATIONAL JOURNAL OF NOVEL RESEARCH AND DEVELOPMENT (IJNRD) | IJNRD.ORG
An International Open Access, Peer-reviewed, Refereed Journal

Synthesis and Analysis of carbon doped shale rock Nanoparticles

by V Vivek IST JNTUK Nanotechnology 2023.

Keywords:
XRD
SEM
EDX
RAMAN

A B S T R A C T

Carbon-based materials have gained significant attention in the field of energy storage due to their unique properties such as high surface area, excellent electrical conductivity, and chemical stability. Shale rock, a sedimentary rock composed mainly of clay minerals, can be a potential source for carbon-based materials. One of the main advantages of using carbon-doped shale rock nanoparticles in energy storage devices is their high specific surface area. The porous structure of these nanoparticles provides a large number of active sites for electrochemical reactions, allowing for efficient charge storage. Additionally, the presence of carbon in the nanoparticles enhances their electrical conductivity, enabling faster electron transfer during charge and discharge cycles. .This abstract focuses on the synthesis of shale rock nanoparticles using a chemical reduction method with HNO3, as well as the doping of graphene into these nanoparticles using the liquid phase exfoliation (LPE) method with propanol. The chemical reduction method involves the use of HNO3 as an oxidizing agent to break down the shale rock into smaller particles. This method offers several advantages, including simplicity, cost-effectiveness, and scalability. The HNO3 reacts with the shale rock, leading to the formation of nanoparticles through a redox reaction. The resulting shale rock nanoparticles exhibit enhanced surface area and reactivity, making them suitable for various applications. Graphene, a two-dimensional carbon allotrope, is known for its exceptional mechanical, electrical, and thermal properties. Doping graphene into shale rock nanoparticles can further enhance their properties and expand their potential applications. The liquid phase exfoliation (LPE) method with propanol is employed for this purpose. Propanol acts as a solvent that facilitates the exfoliation of graphene sheets from graphite and their dispersion into the shale rock nanoparticle suspension. The ultrasonic waves create shear forces that separate the graphene sheets from each other and disperse them uniformly within the nanoparticle suspension. The resulting graphene-doped shale rock nanoparticles exhibit improved conductivity, mechanical strength, and stability. The synthesized shale rock nanoparticles doped with graphene hold great promise in various fields such as energy storage, catalysis, environmental remediation, and electronics. Their increased surface area and unique properties make them suitable for applications such as super capacitors, sensors, adsorbents, and reinforcement materials and The synthesized carbon doped shale rock nanoparticles is dried and calcinated to remove the impurities. The resulting nanoparticles is then characterized using techniques such as Raman spectroscopy, X-ray diffraction (XRD), scanning electron microscopy (SEM) and EDX to determine the rock's composition, mineralogy, and pore structure and morphology of the synthesized carbon doped shale rock nanoparticles.

Introduction

Shale rock nanoparticles refer to the tiny particles that are derived from shale rocks through various processes such as mechanical grinding or chemical treatment. Shale is a fine-grained sedimentary rock composed of clay minerals and organic matter. It is widely distributed around the world and has gained significant attention due to its potential as a source of oil and gas through the process of hydraulic fracturing, also known fracking. In recent years, researchers have started exploring the use of shale rock nanoparticles in various fields, including materials science, environmental remediation, and biotechnology. These nanoparticles possess unique properties that make them attractive for different applications. Understanding the characteristics and potential applications of shale rock nanoparticles is crucial for harnessing their benefits effectively. Shale rock nanoparticles exhibit several distinctive characteristics that make them valuable in different applications. These characteristics include :

Nano-sized Particles: Shale rock nanoparticles have a size range typically below 100 nanometers, which gives them a high surface area-to-volume ratio. This enhanced surface area allows for increased reactivity and interaction with other substances.

Chemical Composition: Shale rocks consist primarily of clay minerals, which contain various elements such as silicon, aluminum, oxygen, and hydrogen. The chemical composition of shale rock nanoparticles can vary depending on the specific shale formation.

Porosity: Shale rocks possess inherent porosity due to their fine-grained nature. This porosity contributes to the storage and transport of fluids within the rock matrix.

Mechanical Strength: Shale rocks are known for their mechanical strength, which translates to the nanoparticles derived from them. This property makes shale rock nanoparticles suitable for applications requiring structural integrity

.**Adsorption Capacity:** Shale rock nanoparticles have a high adsorption capacity due to their porous structure. They can adsorb various substances, including organic compounds, heavy metals, and pollutants, making them useful for environmental remediation.

Effect of Carbon Doping on Internal Structure

The internal structure of shale rock plays a crucial role in determining its mechanical and transport properties. Carbon doping can significantly impact this internal structure and alter various characteristics that influence the behavior of shale rock nanoparticles. Firstly, carbon doping can enhance the porosity of shale rock nanoparticles. The introduction of carbon materials creates additional void spaces within the rock matrix, increasing its overall porosity. This increased porosity can improve the storage capacity of hydrocarbons within the shale formation and facilitate their release during extraction processes. Formation of composites: Graphene and shale rock nanoparticles can form a composite material with a unique internal structure, characterized by the intercalation or exfoliation of graphene layers between the shale rock nanoparticles.

Increased porosity: The addition of graphene can create a more porous internal structure in shale rock nanoparticles, allowing for greater adsorption and reactivity.

Alteration of surface chemistry: Graphene doping can change the surface chemistry of shale rock nanoparticles, potentially affecting their interaction with other materials and environmental conditions.

Enhanced stability: Graphene can improve the stability of shale rock nanoparticles, preventing their aggregation and ensuring their long-term effectiveness in various applications.

Overall, carbon doped shale rock nanoparticles have the potential to revolutionize various industries due to their unique properties and applications. The role of graphene in enhancing the properties of shale rock nanoparticles and the impact of doping on their internal structure have been explored in numerous research studies, paving the way for the development of advanced materials for diverse applications.

Experimental details

The synthesis of shale rock nanoparticles involves several steps, including acid treatment with HNO3 and calcination for removing impurities.

Acid Treatment with HNO3

The first step in the synthesis of shale rock nanoparticles is the acid treatment with nitric acid (HNO3). This process aims to dissolve the mineral components of the shale rock, leaving behind the desired nanoparticles. Nitric acid is commonly used for this purpose due to its strong oxidizing properties and ability to dissolve various minerals.

During the acid treatment, the shale rock is typically crushed into smaller pieces or ground into a fine powder to increase the surface area available for reaction. The shale rock is then mixed with a suitable concentration of nitric acid and allowed to react for a specific period of time. The reaction between shale rock and nitric acid results in the dissolution of minerals such as carbonates, sulfides, and other impurities present in the rock.The acid treatment conditions can vary depending on factors such as the desired particle size, composition of the shale rock, and intended application of the nanoparticles. Optimization of parameters such as acid concentration, reaction time, and temperature is crucial to achieve the desired nanoparticle characteristics.

Filtration and Washing

After the acid treatment, the resulting mixture is typically filtered to separate the dissolved minerals from the remaining solid residue. Filtration can be performed using various methods such as vacuum filtration or centrifugation. The solid residue obtained after filtration contains the desired shale rock nanoparticles.

To remove any residual acids or dissolved impurities adhering to the nanoparticles, washing is usually carried out. This step involves rinsing the solid residue with distilled water multiple times to ensure the removal of any remaining contaminants.

Calcination for Removing Impurities

Calcination is a thermal treatment process used to remove impurities and enhance the properties of nanoparticles. In the context of shale rock nanoparticle synthesis, calcination is employed to eliminate residual organic matter, decompose carbonates, and transform certain mineral phases to more desirable forms.

The calcination process involves heating the washed shale rock nanoparticles at elevated temperatures in a controlled atmosphere. The temperature and duration of calcination depend on factors such as the composition of the shale rock and the desired properties of the nanoparticles. Typically, calcination temperatures range from 500°C to 1000°C. During calcination, organic matter present in the nanoparticles undergoes combustion, resulting in its removal. Additionally, carbonates present in the shale rock decompose, releasing carbon dioxide (CO2) and leaving behind oxides or other desired mineral phases. The calcination process also promotes sintering, which leads to the formation of well-defined nanoparticle structures.

Using Propanol for Synthesis of Graphene LPE Method

Graphite powder preparation: High-quality graphite powder is required for the synthesis of high-quality graphene. The graphite powder is obtained by mechanical milling or grinding of natural graphite or by chemical exfoliation of graphite oxide.

Propanol dispersion: In this step, the graphite powder is dispersed in propanol (C3H7OH), a suitable solvent for the LPE method. The graphite powder is typically sonicated in propanol to break the aggregates and ensure a uniform distribution.

Exfoliation: The graphite-propanol dispersion is subjected to ultra sonication, shear forces, or other mechanical agitation methods to exfoliate the graphite layers. This process separates the layers and forms individual graphene sheets in the solvent.

Collection of exfoliated graphene: After exfoliation, the graphene sheets are collected by filtration, centrifugation, or other separation techniques. The collected graphene can be washed with fresh propanol to remove any residual impurities.

Drying and characterization: The exfoliated graphene is dried under vacuum or at low temperatures to remove the solvent. The resulting graphene is then characterized using techniques such as xrd, sem , edx, raman.

Doping of graphene into shale rock nanoparticles

The doping of graphene into shale rock nanoparticles done using stirring and ultra sonication techniques, they can lead to significant improvements in the properties of shale rock. These improvements can be harnessed in various applications, such as enhanced oil and gas recovery, energy storage, construction materials, and water treatment sectors, resulting nanoparticles were dried and calcinated and then characterized.

3. Results and discussion

Structural analysis by XRD

X-ray diffraction (XRD) analysis was conducted on shale rock samples to determine their crystallographic structure and estimate the average crystalline size of the mineral phases present. The samples, namely Shale Rock Nanoparticles (SHN), Carbon Doped Shale Rock (SHC), Tin Doped Shale Rock (SHT), and Graphene Doped Shale Rock (SHG), exhibited varying average crystalline sizes of 19.212 nm, 14.547 nm, 40.849 nm, and 22.833 nm, respectively. The XRD patterns revealed the presence of minerals such as quartz, feldspar, mica, and clay minerals in the shale rock samples. X-ray diffraction (XRD) analysis is an essential technique for characterizing the crystallographic structure, chemical composition, and physical properties of materials. In this study, the focus was on shale rock samples, which are known for their potential application in energy storage devices due to their unique properties, including their small crystalline size.

Compositional analysis by EDAX

Energy Dispersive X-ray Spectroscopy analysis was carried out for shale rock nanoparticles. The sample is predominantly composed of carbon and oxygen, with weight percentages of 42.47% and 44.66%, respectively. The other elements present in the sample, including sodium, aluminum, silicon, titanium, and iron, are present in trace amounts 1. The sample's composition suggests that it could be used in energy storage applications.

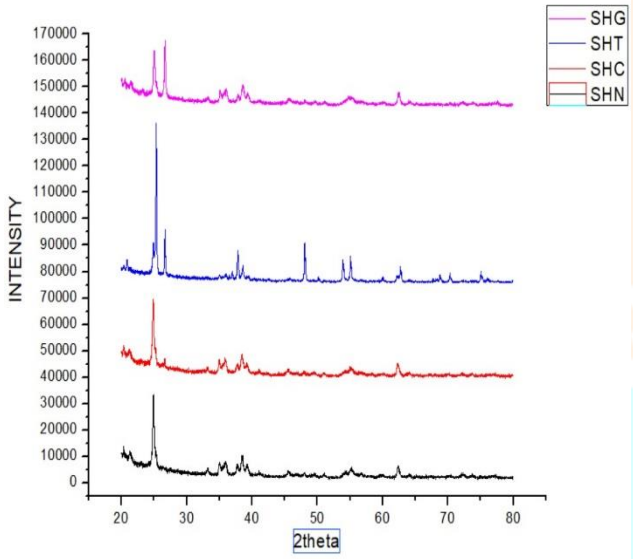

Xrd results of carbon doped shale rock nanoparticles

Shale rock sample	D size
SHN	19.212
SHC	14.547
SHT	40.849
SHG	22.833

Calculated Average Crystalline Size of shale rock nanoparticles

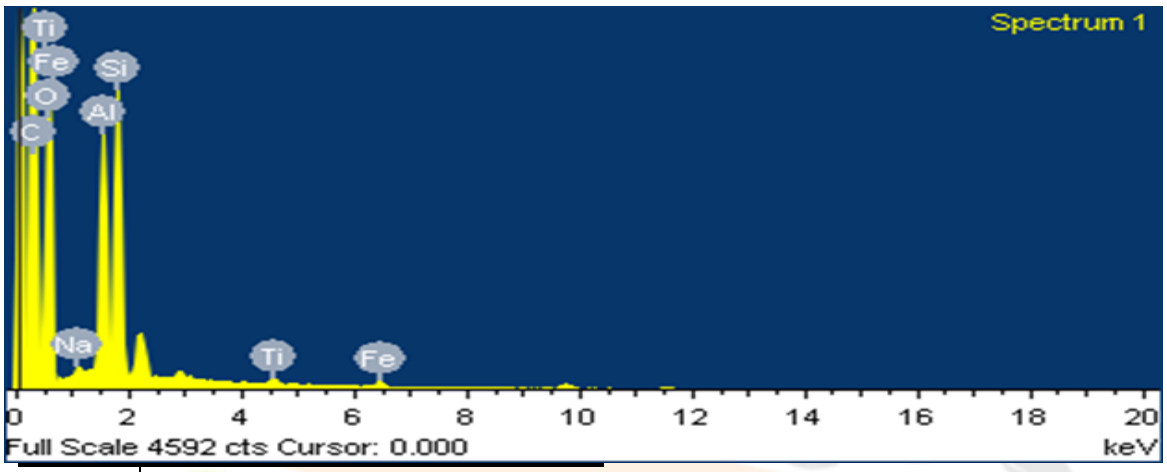

Element	Weight%	Atomic%
C K	42.47	52.15
O K	44.66	41.16
Na K	0.23	0.15
Al K	5.13	2.80
Si K	6.67	3.50
Ti K	0.30	0.09
Fe K	0.54	0.14
Totals	100.00	

EDAX spectrum and analysis of carbon doped shale rock nanoparticles.

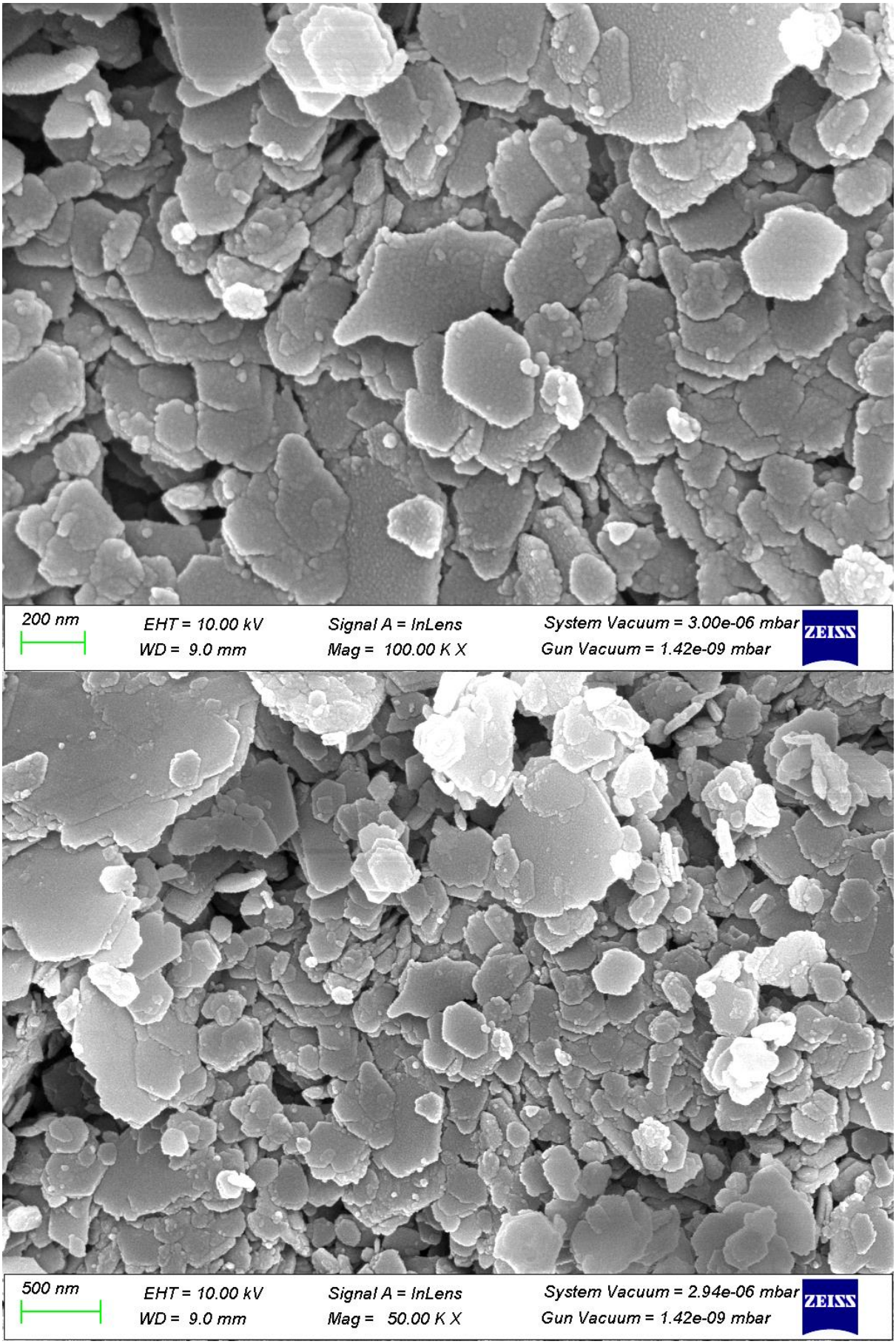

SEM images of prepared carbon doped shale rock nanoparticles at nm range

Morphological analysis by SEM

The scanning electron microscopy (SEM) analysis reveals a complex morphology of aggregated particles with irregular shapes and sizes. These particles exhibit a heterogeneous size distribution and surface texture, indicating a multi-phase formation process. The intricate topography of the particle surfaces suggests potential applications in areas that require high surface area and reactivity. The particles themselves are irregular in shape, with some appearing flatter while others are more elevated, resulting in a rough and uneven surface. Additionally, there is no uniformity in the size of the particles, as they vary greatly, contributing to the overall complex texture of the surface. Based on the scale bar and the number of particles visible in the image, the average particle size is estimated to be around 100 nm. The particles are densely packed together, lacking any distinct pattern or orientation. Furthermore, there is no clear demarcation between individual particles, which indicates possible agglomeration or sintering effects. Agglomeration of the particles may be attributed to attractive forces such as van der Waals forces, electrostatic forces, or chemical bonds, while sintering might be caused by high temperatures or pressures during synthesis or post-treatment. These processes of agglomeration and sintering could potentially impact the porosity, density, and mechanical properties of the sample. The surface of the particles appears rough and porous, displaying varying degrees of roughness and texture. This roughness may be influenced by factors like crystallinity, phase composition, and defect structure of the particles, while the porosity could be affected by gas evolution, solvent evaporation, or phase separation during synthesis or post-treatment. Ultimately, the roughness and porosity of the surface play a crucial role in determining the surface area, reactivity, and catalytic activity of the sample. For a comprehensive characterization of the sample, it is recommended to employ additional techniques such as X-ray diffraction, energy-dispersive X-ray spectroscopy, or transmission electron microscopy.

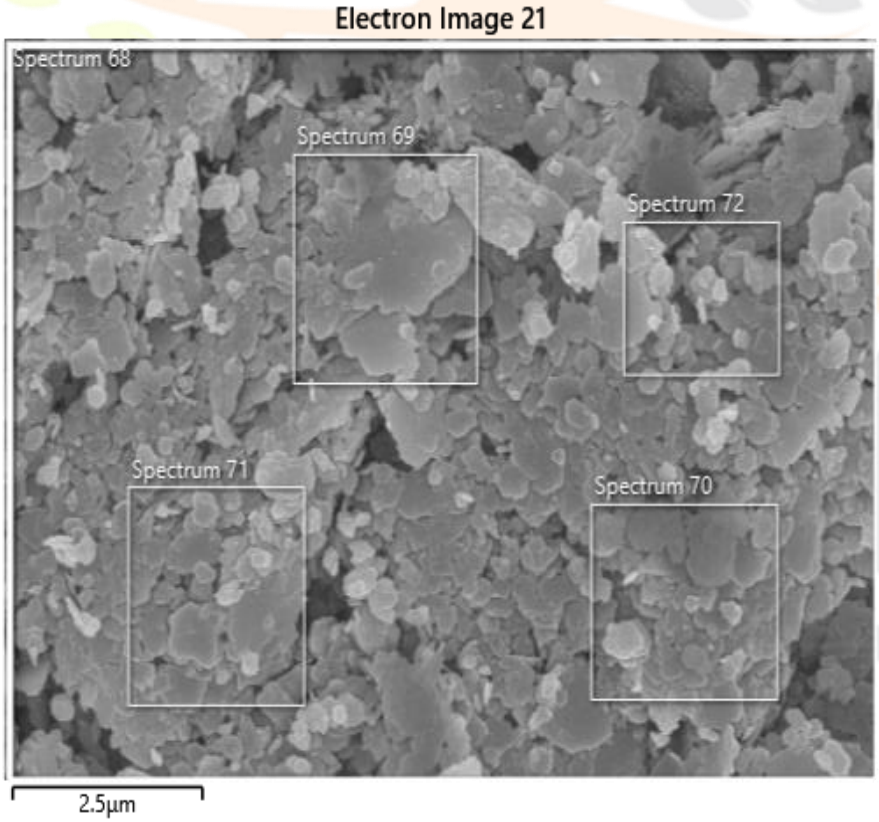

Carbon doped shale rock nanoparticles electron image

Vibrational analysis by Raman Spectroscopy:

Raman spectroscopy is a non-destructive analytical technique used to study vibrational, rotational, and other low-frequency modes in a system. It provides detailed information about chemical structure, crystallinity, and molecular interactions. This technique is based on the Raman effect, which involves the inelastic scattering of photons by molecules. When light interacts with a molecule, most of the scattered light has the same energy (frequency) as the incident light (Rayleigh scattering). However, a small fraction of the scattered light has different energies due to interactions with molecular vibrations or rotations. This shift in energy provides valuable information about the molecular composition and structure of the sample. The Raman spectrum for each Ψ value is done with excitation wavelength 1000 nm using BW TEK Mini Raman instrument. In the Raman spectrum of shale rock nanoparticles, showed three strong peaks around 780, 790, and 850 cm, and two weak bands at 900 and 925 cm (Fig. 5.8) are observed. The peaks at 825 cm^{21} and 850 cm^{21} in the Raman spectrum of shale rock nanoparticles are related to the doping of carbon nanoparticles and shows change in shift. Based on the Raman analysis, there is a noticeable shift and change in the peaks across different samples (S3,S2, S1, S). The peaks represent vibrational modes of molecules in the sample. A shift in peak positions indicates a change in molecular or crystal structure. For instance, the peak near 800 on the x-axis for SHN shifts to higher wavenumbers for S1 Dar and continues shifting for S2 and S3. This could be due to changes or variations in chemical composition, stress/strain levels or other structural modifications. The intensity of peaks also varies among samples; this can be attributed to differences in concentration or orientation of molecules contributing to specific vibrational modes. Each spectrum has distinct peaks indicating different molecular structures or compositions. There are notable shifts and changes in peak intensities among these spectra. These changes can reveal compressive/tensile stresses in the sample, variations in crystallinity, and the amount of material respectively

.

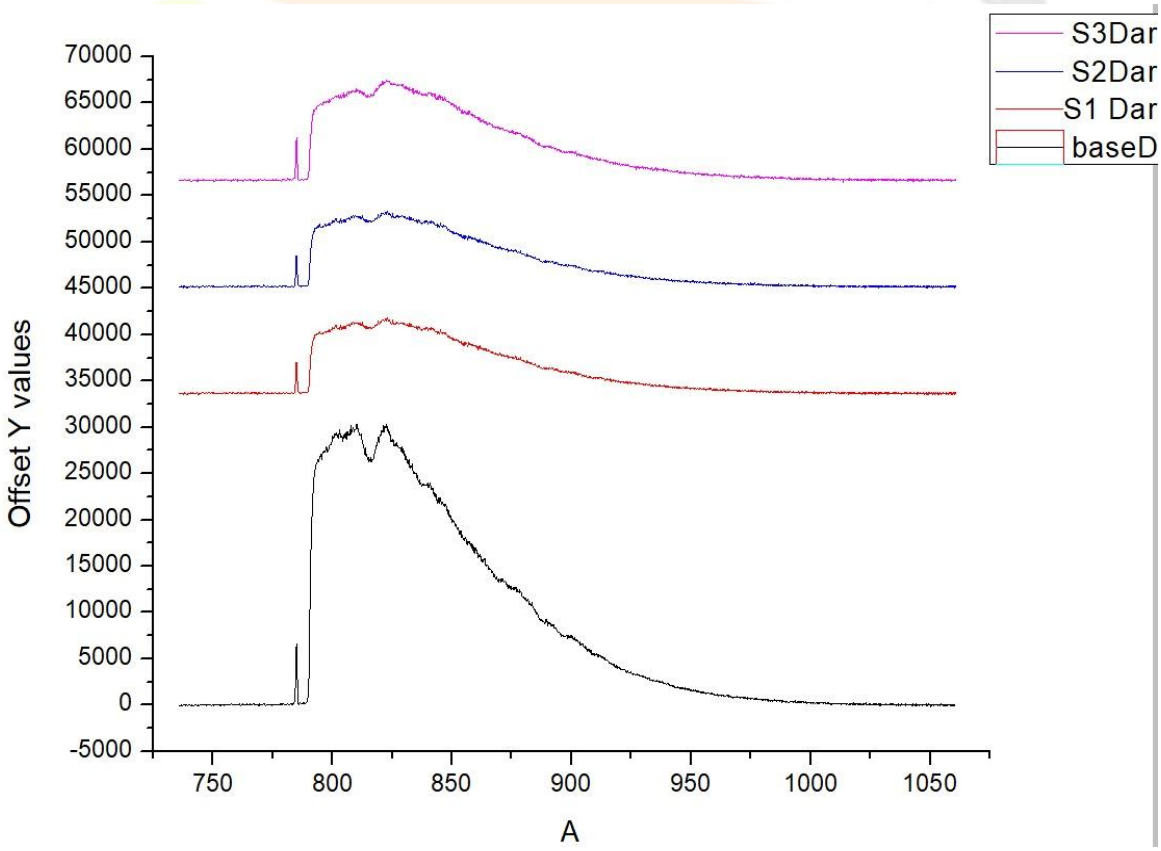

Vibrational Analysis by Raman spectroscopy

Conclusion

In conclusion, successfully synthesized carbon-doped shale rock nanoparticles using a chemical reduction method from shale rock and ultra sonication for carbon doping. Graphene oxide was also synthesized using propanol with the LDE method, Two nanoparticles were successfully doped , carbon-doped shale rock nanoparticles were obtained ,Characterization analysis revealed that the synthesized nanoparticles consisted of a mixture of elements, including c, o ,na, fe, and Al, Si. XRD analysis confirmed a crystalline structure, with average crystalline sizes of 19 nm for shale rock and 22.8 nm for carbon-doped shale rock. SEM images displayed a hexagonal structure with densely packed, irregularly shaped particles resembling flower petals or scales. EDX results indicated the presence of carbon, oxygen, sodium, aluminum, silicon, titanium, and iron in the material. Raman spectroscopy analysis revealed a complex molecular structure, with the highest peak appearing around 800 cm-1 for shale rock nanoparticles and a Raman shift at 780 cm-1. These findings demonstrate the potential conductivity and stability of the synthesized nanoparticles. The irregular shapes and sizes of the particles increase the surface area and reactivity of the material, which can enhance the charge storage and transfer processes. The rough and porous surface of the particles provide more active sites and channels for the electrolyte ions to access and interact with the material, which can improve the capacitance and rate performance of the material. The agglomeration and sintering of the particles create a dense and compact structure, which can reduce the internal resistance and increase the conductivity of the material. These morphological features can contribute to the high energy density and power density of the material, making it suitable for super capacitors and other energy storage devices.

References

1. Fang, B.; Chang, D.; Xu, Z.; Gao, C. A Review on Graphene Fibers: Expectations, Advances, and Prospects. *Adv. Mater.* **2020**, *32*, 1902664. [Google Scholar] [CrossRef]
2. Hass, J.; De Heer, W.A.A.; Conrad, E.H. The growth and morphology of epitaxial multilayer graphene. *J. Phys. Condens. Matter* **2008**, *20*, 323202. [Google Scholar] [CrossRef]
3. Yoo, E.; Kim, J.; Hosono, E.; Zhou, H.-S.; Kudo, T.; Honma, I. Large Reversible Li Storage of Graphene Nanosheet Families for Use in Rechargeable Lithium Ion Batteries. *Nano Lett.* **2008**, *8*, 2277–2282. [Google Scholar] [CrossRef]
4. Stoller, M.D.; Park, S.; Zhu, Y.; An, J.; Ruoff, R.S. Graphene-Based Ultracapacitors. *Nano Lett.* **2008**, *8*, 3498–3502. [Google Scholar] [CrossRef] [PubMed]
5. Kou, R.; Shao, Y.; Wang, D.; Engelhard, M.H.; Kwak, J.H.; Wang, J.; Viswanathan, V.V.; Wang, C.; Lin, Y.; Wang, Y.; et al. Enhanced activity and stability of Pt catalysts on functionalized graphene sheets for electrocatalytic oxygen reduction. *Electrochem. Commun.* **2009**, *11*, 954–957. [Google Scholar] [CrossRef]
6. Wu, J.; Becerril, H.A.; Bao, Z.; Liu, Z.; Chen, Y.; Peumans, P. Organic solar cells with solution-processed graphene transparent electrodes. *Appl. Phys. Lett.* **2008**, *92*, 263302. [Google Scholar] [CrossRef][Green Version]
7. Sun, S.; Gao, L.; Liu, Y. Enhanced dye-sensitized solar cell using graphene-TiO_2 photoanode prepared by heterogeneous coagulation. *Appl. Phys. Lett.* **2010**, *96*, 083113. [Google Scholar] [CrossRef]
8. Balandin, A.A.; Ghosh, S.; Bao, W.; Calizo, I.; Teweldebrhan, D.; Miao, F.; Lau, C.N. Superior Thermal Conductivity of Single-Layer Graphene. *Nano Lett.* **2008**, *8*, 902–907. [Google Scholar] [CrossRef]
9. Service, R.F. Materials science. Carbon sheets an atom thick give rise to graphene dreams. *Science* **2009**, *324*, 875–877. [Google Scholar] [PubMed]
10. Lee, C.; Wei, X.; Kysar, J.W.; Hone, J. Measurement of the Elastic Properties and Intrinsic Strength of Monolayer Graphene. *Science* **2008**, *321*, 385–388. [Google Scholar] [CrossRef]
11. Zheng, P.; Wu, N. Fluorescence and Sensing Applications of Graphene Oxide and Graphene Quantum Dots: A Review. *Chem.—Asian J.* **2017**, *12*, 2343–2353. [Google Scholar] [CrossRef] [PubMed]
12. Allen, M.J.; Tung, V.C.; Kaner, R.B. Honeycomb Carbon: A Review of Graphene. *Chem. Rev.* **2009**, *110*, 132–145. [Google Scholar] [CrossRef]
13. Enoki, T.; Endo, M.; Suzuki, M. *Graphite Intercalation Compounds and Applications*; Oxford University Press: New York, NY, USA, 2003; p. 452. [Google Scholar]
14. Choi, W.; Lahiri, I.; Seelaboyina, R.; Kang, Y.S. Synthesis of Graphene and Its Applications: A Review. *Crit. Rev. Solid State Mater. Sci.* **2010**, *35*, 52–71. [Google Scholar] [CrossRef]
15. Nimbalkar, A.; Kim, H. Opportunities and Challenges in Twisted Bilayer Graphene: A Review. *Nano-Micro Lett.* **2020**, *12*, 1–20. [Google Scholar] [CrossRef]
16. Bacon, M.; Bradley, S.J.; Nann, T. Graphene Quantum Dots. *Part. Part. Syst. Charact.* **2014**, *31*, 415–428. [Google Scholar] [CrossRef]
17. Geim, A.K.; Novoselov, K.S. The rise of graphene. *Nat. Mater.* **2007**, *6*, 183–191. [Google Scholar] [CrossRef] [PubMed]
18. Chen, J.-H.; Jang, C.; Xiao, S.; Ishigami, M.; Fuhrer, M.S. Intrinsic and extrinsic performance limits of graphene devices on SiO2. *Nat. Nanotechnol.* **2008**, *3*, 206–209. [Google Scholar] [CrossRef]
19. Balandin, A.A. Phononics of Graphene and Related Materials. *ACS Nano* **2020**, *14*, 5170–5178. [Google Scholar] [CrossRef]
20. Rhee, K.Y. Electronic and Thermal Properties of Graphene. *Nanomaterials* **2020**, *10*, 926. [Google Scholar] [CrossRef]
21. Guo, X.; Cheng, S.; Cai, W.; Zhang, Y.; Zhang, X.A. A review of carbon-based thermal interface materials: Mechanism, thermal measurements and thermal properties. *Mater. Des.* **2021**, *209*, 109936. [Google Scholar] [CrossRef]
22. Reina, A.; Jia, X.; Ho, J.; Nezich, D.; Son, H.; Bulovic, V.; Dresselhaus, M.S.; Kong, J. Large Area, Few-Layer Graphene Films on Arbitrary Substrates by Chemical Vapor Deposition. *Nano Lett.* **2009**, *9*, 30–35. [Google Scholar] [CrossRef]
23. Li, X.; Cai, W.; An, J.; Kim, S.; Nah, J.; Yang, D.; Piner, R.; Velamakanni, A.; Jung, I.; Tutuc, E.; et al. Large-Area Synthesis of High-Quality and Uniform Graphene Films on Copper Foils. *Science* **2009**, *324*, 1312–1314. [Google Scholar] [CrossRef] [PubMed][Green Version]
24. Shams, S.S.; Zhang, R.; Zhu, J. Graphene synthesis: A Review. *Mater. Sci.-Pol.* **2016**, *33*, 566–578. [Google Scholar] [CrossRef][Green Version]
25. Muñoz, R.; Gómez-Aleixandre, C. Review of CVD Synthesis of Graphene. *Chem. Vap. Depos.* **2013**, *19*, 297–322. [Google Scholar] [CrossRef][Green Version]
26. Emtsev, K.V.; Bostwick, A.; Horn, K.; Jobst, J.; Kellogg, G.L.; Ley, L.; McChesney, J.; Ohta, T.; Reshanov, S.A.; Röhrl, J.; et al. Towards wafer-size graphene layers by atmospheric pressure graphitization of silicon carbide. *Nat. Mater.* **2009**, *8*, 203–207. [Google Scholar] [CrossRef] [PubMed]
27. Zhang, R.; Dong, Y.; Kong, W.; Han, W.; Tan, P.-H.; Liao, Z.-M.; Wu, X.; Yu, D. Growth of large domain epitaxial graphene on the C-face of SiC. *J. Appl. Phys.* **2012**, *112*, 104307. [Google Scholar] [CrossRef][Green Version]
28. Stankovich, S.; Dikin, D.A.; Piner, R.D.; Kohlhaas, K.A.; Kleinhammes, A.; Jia, Y.; Wu, Y.; Nguyen, S.; Ruoff, R.S. Synthesis of graphene-based

nanosheets via chemical reduction of exfoliated graphite oxide. *Carbon* **2007**, *45*, 1558–1565. [Google Scholar] [CrossRef]

29. Schniepp, H.C.; Li, J.-L.; McAllister, M.J.; Sai, H.; Herrera-Alonso, M.; Adamson, D.H.; Prud'Homme, R.K.; Car, R.; Saville, D.A.; Aksay, I.A. Functionalized Single Graphene Sheets Derived from Splitting Graphite Oxide. *J. Phys. Chem. B* **2006**, *110*, 8535–8539. [Google Scholar] [CrossRef][Green Version]
30. Park, S.; Ruoff, R.S. Chemical methods for the production of graphenes. *Nat. Nanotechnol.* **2009**, *4*, 217–224. [Google Scholar] [CrossRef]